

A small-molecule inhibitor of the NLRP3 inflammasome for the treatment of inflammatory diseases

Rebecca C Coll^{1,2}, Avril A B Robertson², Jae Jin Chae³, Sarah C Higgins¹, Raúl Muñoz-Planillo⁴, Marco C Inserra^{2,5}, Irina Vetter^{2,5}, Lara S Dungan¹, Brian G Monks⁶, Andrea Stutz⁶, Daniel E Croker², Mark S Butler², Moritz Haneklaus¹, Caroline E Sutton¹, Gabriel Núñez⁴, Eicke Latz⁶⁻⁸, Daniel L Kastner³, Kingston H G Mills¹, Seth L Masters⁹, Kate Schroder², Matthew A Cooper² & Luke A J O'Neill¹

The NOD-like receptor (NLR) family, pyrin domain-containing protein 3 (NLRP3) inflammasome is a component of the inflammatory process, and its aberrant activation is pathogenic in inherited disorders such as cryopyrin-associated periodic syndrome (CAPS) and complex diseases such as multiple sclerosis, type 2 diabetes, Alzheimer's disease and atherosclerosis. We describe the development of MCC950, a potent, selective, small-molecule inhibitor of NLRP3. MCC950 blocked canonical and noncanonical NLRP3 activation at nanomolar concentrations. MCC950 specifically inhibited activation of NLRP3 but not the AIM2, NLRC4 or NLRP1 inflammasomes. MCC950 reduced interleukin-1 β (IL-1 β) production *in vivo* and attenuated the severity of experimental autoimmune encephalomyelitis (EAE), a disease model of multiple sclerosis. Furthermore, MCC950 treatment rescued neonatal lethality in a mouse model of CAPS and was active in *ex vivo* samples from individuals with Muckle-Wells syndrome. MCC950 is thus a potential therapeutic for NLRP3-associated syndromes, including autoinflammatory and autoimmune diseases, and a tool for further study of the NLRP3 inflammasome in human health and disease.

The NLR family protein NLRP3 is an intracellular signaling molecule that senses many pathogen-derived, environmental and host-derived factors¹. Upon activation, NLRP3 binds to apoptosis-associated speck-like protein containing a CARD (ASC). ASC in turn interacts with the cysteine protease caspase-1 to form a complex termed the inflammasome. This results in the activation of caspase-1, which cleaves the proinflammatory cytokines IL-1 β and IL-18 to their active forms and mediates a type of inflammatory cell death known as pyroptosis². Other intracellular pattern recognition receptors (PRRs) are also capable of forming inflammasomes. These include other NLR family members such as NLRP1 and NLRC4, as well as non-NLR PRRs such as the double-stranded DNA (dsDNA) sensors absent in melanoma 2 (AIM2) and interferon, gamma inducible protein 16 (IFI16)³. NLRP3-dependent IL-1 β processing can also be activated by an indirect, non-canonical pathway downstream of caspase-11 (ref. 4).

The inherited CAPSs Muckle-Wells syndrome (MWS), familial cold autoinflammatory syndrome and neonatal-onset multisystem inflammatory disease are caused by gain-of-function mutations in NLRP3, thus defining NLRP3 as a critical component of the inflammatory process⁵. NLRP3 has also been implicated in the pathogenesis of a number of complex diseases, notably including metabolic disorders such as type 2 diabetes, atherosclerosis, obesity and gout⁶.

A role for NLRP3 in diseases of the central nervous system is emerging, and lung diseases have also been shown to be influenced by NLRP3 (ref. 7). Furthermore, NLRP3 has a role in the development of liver disease⁸, kidney disease⁹ and aging¹⁰. Many of these associations were defined using *Nlrp3*^{-/-} mice, but there have also been insights into the specific activation of NLRP3 in these diseases. In type 2 diabetes, the deposition of islet amyloid polypeptide in the pancreas activates NLRP3 and IL-1 β signaling, which results in cell death and inflammation¹¹.

Current treatments for NLRP3-related diseases include biologic agents that target IL-1. These are the recombinant IL-1 receptor antagonist anakinra, the neutralizing IL-1 β antibody canakinumab and the soluble decoy IL-1 receptor rilonacept. This approach has proven successful in the treatment of CAPS, and these biologic agents have been used in clinical trials for other IL-1 β -associated diseases¹². Several small molecules have been shown to inhibit the NLRP3 inflammasome. Glyburide inhibits IL-1 β production at micromolar concentrations in response to the activation of NLRP3 but not NLRC4 or NLRP1 (ref. 13). We previously described a small molecule capable of inhibiting both NLRP3 and AIM2 at micromolar concentrations; this molecule was initially incorrectly termed CRID3 but was in fact a Bayer compound that is a cysteinyl leukotriene-receptor antagonist¹⁴.

¹School of Biochemistry and Immunology, Trinity Biomedical Sciences Institute, Trinity College Dublin, Dublin, Ireland. ²Institute for Molecular Bioscience, University of Queensland, Brisbane, Australia. ³Inflammatory Disease Section, Medical Genetics Branch, National Human Genome Research Institute, National Institutes of Health, Bethesda, Maryland, USA. ⁴Department of Pathology and Comprehensive Cancer Center, University of Michigan Medical School, Ann Arbor, Michigan, USA. ⁵School of Pharmacy, University of Queensland, Brisbane, Australia. ⁶Institute of Innate Immunity, University Hospital, University of Bonn, Bonn, Germany. ⁷Department of Infectious Diseases and Immunology, University of Massachusetts Medical School, Worcester, Massachusetts, USA. ⁸German Center for Neurodegenerative Diseases, Bonn, Germany. ⁹The Walter and Eliza Hall Institute of Medical Research, Parkville, Australia. Correspondence should be addressed to L.A.J.O'N. (laoneill@tcd.ie) or M.A.C. (m.cooper@imb.uq.edu.au).

Received 23 October 2014; accepted 22 January 2015; published online 16 February 2015; doi:10.1038/nm.3806

Other purported NLRP3 inhibitors include parthenolide¹⁵, 3,4-methylenedioxy- β -nitrostyrene¹⁶ and dimethyl sulfoxide (DMSO)¹⁷, although these agents have limited potency and are nonspecific.

In 2001 a number of diarylsulfonylurea-containing compounds were identified as novel IL-1 β processing inhibitors¹⁸. In this study we investigated one of these that we have termed MCC950 (ref. 19). The synthesis and chemical structure of MCC950 are described in the Online Methods, **Supplementary Table 1** and **Supplementary Figures 1–5**. Here we describe how MCC950 is a highly potent specific NLRP3 inhibitor that was observed to be active *in vivo* in multiple NLRP3-dependent mouse models and in *ex vivo* samples from individuals with CAPS.

RESULTS

MCC950 inhibits canonical and noncanonical NLRP3 activation

The effect of MCC950 (**Fig. 1a**) on NLRP3 inflammasome activation was tested in mouse bone marrow-derived macrophages (BMDMs), human monocyte-derived macrophages (HMDMs) and human peripheral blood mononuclear cells (PBMCs). Cells were first primed with lipopolysaccharide (LPS), then pretreated with MCC950 and lastly stimulated with the NLRP3 stimulus ATP. Treating cells with

nanomolar concentrations of MCC950 dose-dependently inhibited the release of IL-1 β in BMDMs (**Fig. 1b**), HMDMs (**Supplementary Fig. 6a**) and PBMCs (**Supplementary Fig. 6b**). The half-maximal inhibitory concentration (IC₅₀) of MCC950 was approximately 7.5 nM in BMDMs, and it was very similar in HMDMs (IC₅₀ = 8.1 nM). LPS-dependent tumor necrosis factor- α (TNF- α) secretion was not impaired by MCC950 (**Fig. 1b** and **Supplementary Fig. 6a,b**), which demonstrates that the inhibition of IL-1 β secretion was specific.

The amount of caspase-1 p10 (an autoprocessed fragment of caspase-1) was dose-dependently reduced in supernatants from MCC950-treated BMDMs and PBMCs (**Fig. 1c** and **Supplementary Fig. 6c**), suggesting that MCC950 inhibits the activation of caspase-1 by NLRP3. Correspondingly, the processing of IL-1 β was inhibited by MCC950 (**Fig. 1c** and **Supplementary Fig. 6c**). MCC950 treatment did not consistently affect the expression of pro-IL-1 β or pro-caspase-1 in cell lysates (**Fig. 1c** and **Supplementary Fig. 6c**). Similarly, treatment with glyburide inhibited caspase-1 activation and IL-1 β processing in these assays (**Fig. 1c** and **Supplementary Fig. 6c**).

We also tested MCC950 with other NLRP3 stimuli. LPS-primed BMDMs were treated with MCC950 and stimulated with the ionophore nigericin²⁰ (**Fig. 1d–g**) or monosodium urate crystals (MSU)²¹

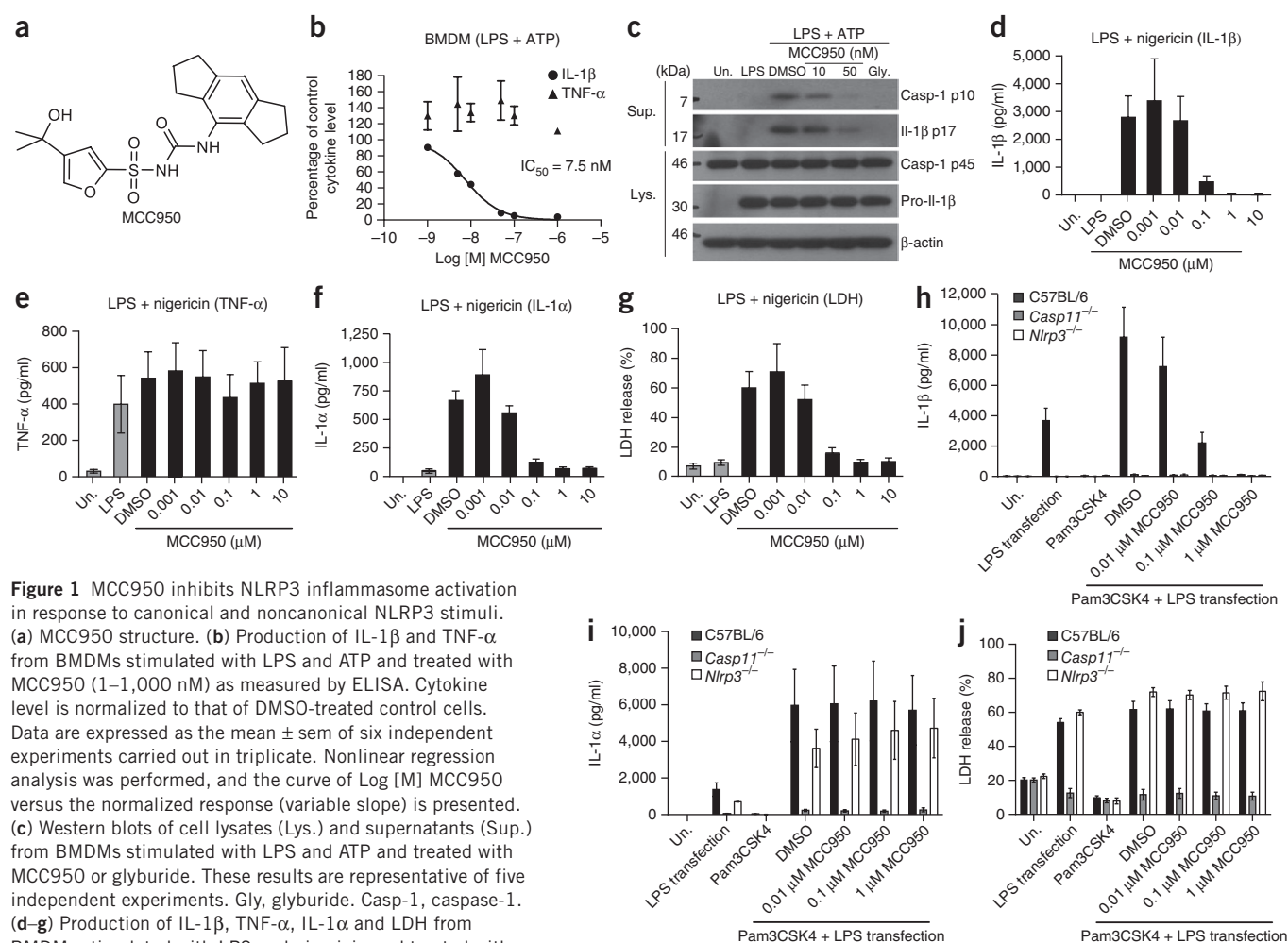
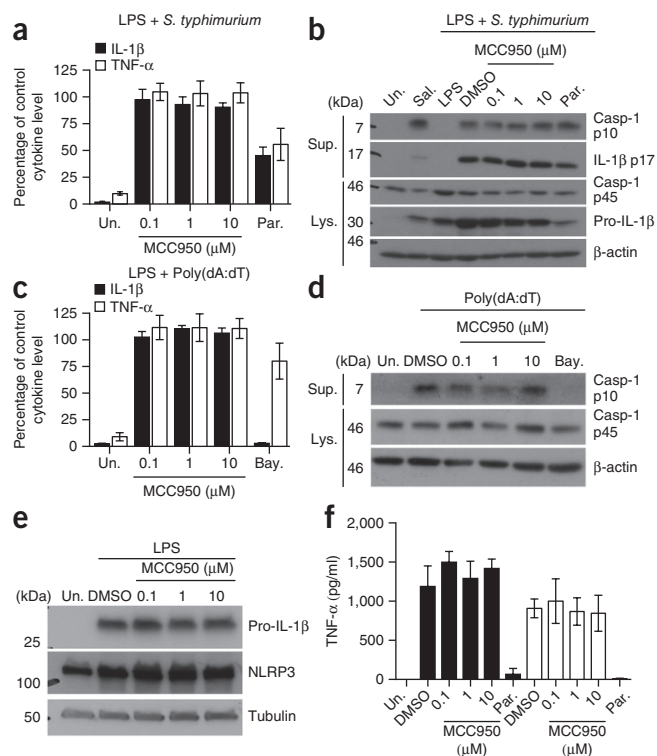


Figure 1 MCC950 inhibits NLRP3 inflammasome activation in response to canonical and noncanonical NLRP3 stimuli. **(a)** MCC950 structure. **(b)** Production of IL-1 β and TNF- α from BMDMs stimulated with LPS and ATP and treated with MCC950 (1–1,000 nM) as measured by ELISA. Cytokine level is normalized to that of DMSO-treated control cells. Data are expressed as the mean \pm sem of six independent experiments carried out in triplicate. Nonlinear regression analysis was performed, and the curve of Log [M] MCC950 versus the normalized response (variable slope) is presented. **(c)** Western blots of cell lysates (Lys.) and supernatants (Sup.) from BMDMs stimulated with LPS and ATP and treated with MCC950 or glyburide. These results are representative of five independent experiments. Gly, glyburide. Casp-1, caspase-1. **(d–g)** Production of IL-1 β , TNF- α , IL-1 α and LDH from BMDMs stimulated with LPS and nigericin and treated with MCC950 as measured by ELISA (**d–f**) and LDH assay (**g**). Data are expressed as the mean \pm sem of three independent experiments carried out in triplicate. Un, unstimulated. **(h–j)** Production of IL-1 β , IL-1 α and LDH from BMDMs from the indicated genotypes stimulated with Pam3CSK4 and transfected LPS and treated with MCC950 as measured by ELISA (**h,i**) and LDH assay (**j**). Data are expressed as the mean \pm sem of three (*Nlrp3*^{-/-}), four (*Casp11*^{-/-}) or six (C57BL/6) independent experiments.

Figure 2 MCC950 does not inhibit NLRC4, AIM2, TLR signaling or priming of NLRP3. **(a)** Production of IL-1 β and TNF- α (as measured by ELISA) from BMDMs stimulated with LPS and *S. typhimurium* and treated with MCC950 and parthenolide (Par.). Cytokine level is normalized to that of DMSO-treated control cells. Data are expressed as the mean \pm sem of four independent experiments carried out in triplicate. **(b)** Western blots of cell lysates and supernatants from BMDMs stimulated with LPS and *S. typhimurium* and treated with MCC950 and parthenolide. These results are representative of four independent experiments. Sal., *S. typhimurium*. **(c)** Production of IL-1 β and TNF- α (as measured by ELISA) from BMDMs stimulated with LPS and transfected Poly(dA:dT) and treated with MCC950 and Bayer compound (Bay.). Cytokine level is normalized to that of DMSO-treated control cells. Data are expressed as the mean \pm sem of five independent experiments carried out in triplicate. **(d)** Western blots of cell lysates and supernatants from BMDMs stimulated with LPS and transfected Poly(dA:dT) and treated with MCC950 and Bayer compound. These results are representative of two independent experiments. **(e)** Western blots of cell lysates from BMDMs treated with MCC950 and stimulated with LPS (4 h). These results are representative of three independent experiments. **(f)** Production of TNF- α (as measured by ELISA) from BMDMs treated with MCC950 and parthenolide and stimulated with LPS or Poly(A:U). Data shown represent the mean cytokine level \pm sd from triplicate determinations and are representative of three independent experiments.

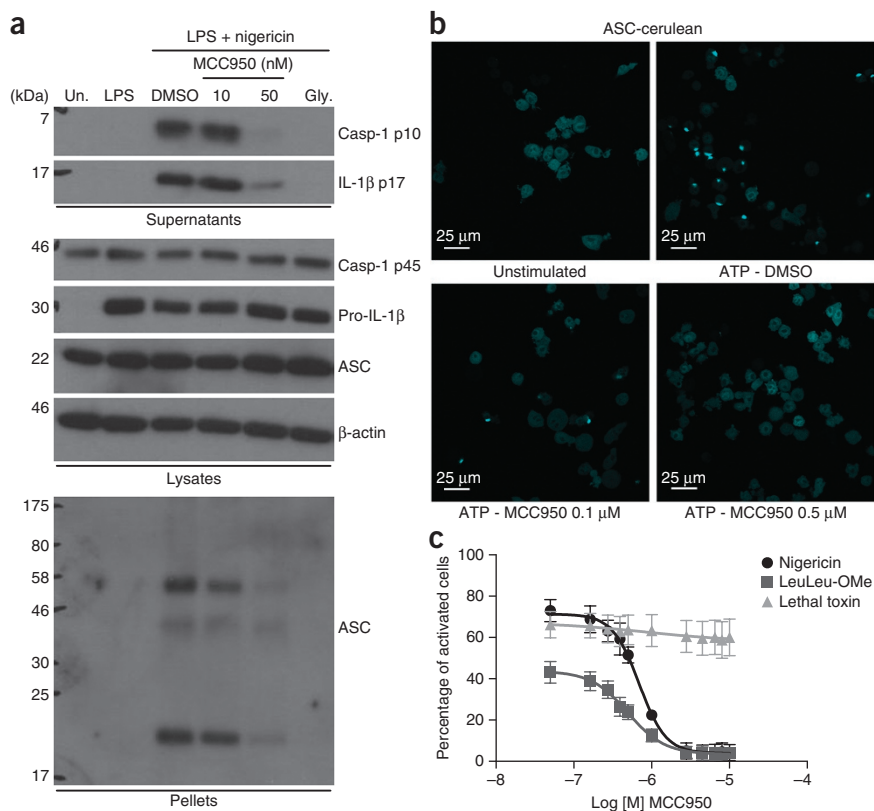
(Supplementary Fig. 6d–g). MCC950 inhibited IL-1 β release in response to both stimuli (Fig. 1d and Supplementary Fig. 6d) but did not block TNF- α secretion (Fig. 1e and Supplementary Fig. 6g). The release of IL-1 α and lactate dehydrogenase (LDH) induced by nigericin was potently blocked by MCC950 (Fig. 1f,g), but MCC950 did not block the release of IL-1 α or LDH in response to MSU (Supplementary Fig. 6e,f). It was previously demonstrated that MSU induced IL-1 α and LDH release are both independent of NLRP3 (refs. 22,23). The effects of MCC950 on the release of IL-1 α and LDH (Fig. 1f,g and Supplementary Fig. 6e,f) thus suggest that MCC950 specifically blocks NLRP3-dependent pyroptotic cell death. In contrast to the



results of short-term stimulation with LPS (3 h), PBMCs seeded at high density and stimulated with LPS alone for 24 h activate caspase-1 and secrete IL-1 β as a result of endogenous ATP release²⁴. We found that MCC950 also dose-dependently inhibited the secretion of IL-1 β but not TNF- α in this assay (Supplementary Fig. 6h,i).

Gram-negative bacteria and intracellular LPS are sensed by a noncanonical pathway that results in caspase-11-dependent pyroptotic cell death and IL-1 β production⁴. NLRP3 is required for IL-1 β processing by the noncanonical pathway^{25,26}. We activated caspase-11 in BMDMs primed with the TLR2/1 ligand Pam3CSK4 and transfected with LPS²⁶ (Fig. 1h–j). By using *Casp11*^{-/-} and *Nlrp3*^{-/-} BMDMs, we confirmed that IL-1 β secretion was dependent on both NLRP3 and caspase-11 and that the release of LDH

Figure 3 MCC950 blocks NLRP3-dependent ASC oligomerization. **(a)** Western blots of cell lysates, supernatants and cross-linked cytosolic pellets from BMDMs stimulated with LPS and nigericin and treated with MCC950 and parthenolide. These results are representative of three independent experiments. **(b)** Live-cell imaging of ASC-cerulean cells treated with MCC950 and stimulated with ATP. At least five different images were taken of each condition at an original magnification of $\times 40$. Results are representative of three independent experiments. **(c)** The percentage of ASC-cerulean cells containing an ASC speck after treatment with MCC950 (0.05–10 μ M) and stimulation with nigericin, LeuLeu-OME or lethal toxin. Data shown represent the mean \pm sd from triplicate measurements.



and IL-1 α was not dependent on NLRP3 in this assay (Fig. 1h–j). We found that pretreatment of wild-type (WT) cells with MCC950 before transfection with LPS resulted in a dose-dependent inhibition of IL- β release (Fig. 1h) but had no effect on IL-1 α secretion (Fig. 1i) or LDH release (Fig. 1j). We therefore concluded that MCC950 specifically blocks caspase-11-directed NLRP3 activation and IL-1 β secretion upon stimulation of the noncanonical pathway.

MCC950 does not inhibit NLRC4, AIM2, NLRP3 priming or Toll-like receptor signaling

Next we examined whether MCC950 could inhibit the activation of other inflammasome complexes. NLRC4-stimulated secretion of IL-1 β and TNF- α (as activated by *Salmonella typhimurium*²⁷) was not inhibited by MCC950 even at a concentration of 10 μ M (Fig. 2a). MCC950 did not inhibit caspase-1 activation or IL-1 β processing in response to *S. typhimurium* (Fig. 2b). The expression of pro-caspase-1 and pro-IL-1 β in cell lysates was not substantially affected by MCC950 treatment (Fig. 2b). Parthenolide has previously been shown to inhibit NLRC4-dependent caspase-1 activation¹⁵, although it did not do so in these experiments (Fig. 2b). Parthenolide attenuated the secretion of IL-1 β and TNF- α (Fig. 2a) and the expression of pro-IL-1 β (Fig. 2b), which suggests that its inhibitory effect is on the nuclear factor- κ B pathway rather than on caspase-1 activation by NLRC4.

The effect of MCC950 on the non-NLR AIM2 inflammasome was examined by transfecting BMDMs with the dsDNA analog Poly(dA:dT)^{28–31}. MCC950 treatment did not attenuate the secretion of IL-1 β or TNF- α from BMDMs in response to stimulation with LPS and Poly(dA:dT) (Fig. 2c). However, IL-1 β secretion, but not TNF- α secretion, was inhibited in cells treated with the Bayer cysteinyl leukotriene-receptor antagonist 1-(5-carboxy-2[3-[4-(3-cyclohexylpropoxy)phenyl]propoxy]benzoyl)piperidine-4-carboxylic acid, as has

been described¹⁴ (Fig. 2c). The Bayer compound, but not MCC950, inhibited Poly(dA:dT)-stimulated caspase-1 activation (Fig. 2d).

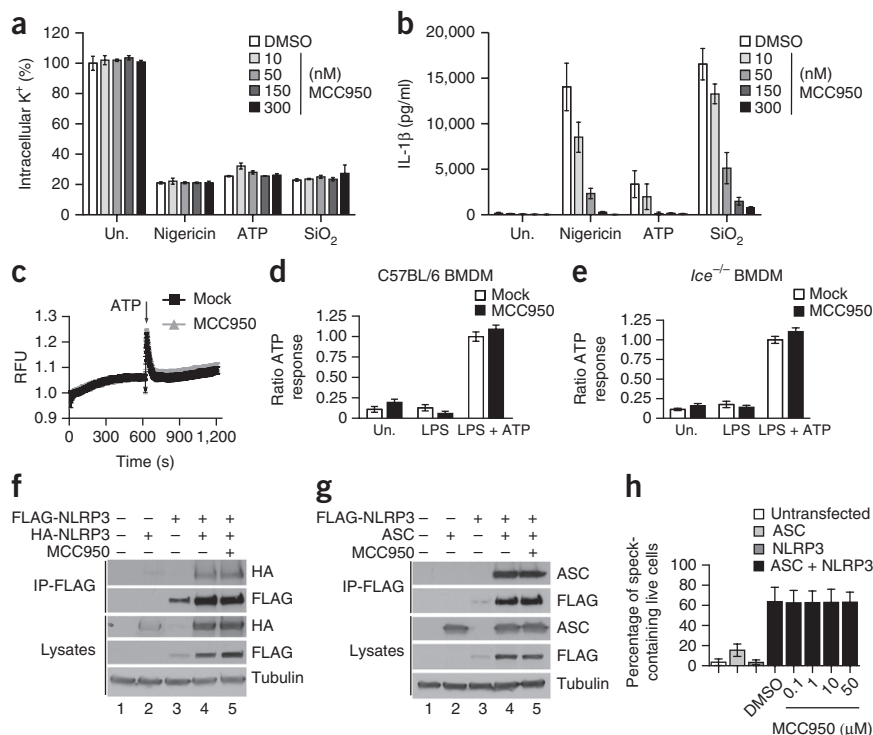
We then specifically examined whether MCC950 influenced the priming phase of NLRP3 activation. BMDMs were pretreated with MCC950 or parthenolide and then stimulated with TLR ligands (Fig. 2e,f). As shown in Figure 2e, the LPS-stimulated induction of NLRP3 and pro-IL-1 β was not affected by MCC950 pretreatment. Likewise, MCC950 did not affect LPS- or Poly(A:U)-induced TNF- α secretion (Fig. 2f). In contrast, parthenolide, which is an inhibitor of I κ B kinase- β (ref. 32), abrogated both TLR4- and TLR3-stimulated TNF- α production. Together these data demonstrate that MCC950 does not inhibit TLR signaling or the priming phase of NLRP3 activation.

MCC950 blocks NLRP3-induced ASC oligomerization

We next examined the formation of NLRP3-dependent ASC oligomers, a key event in NLRP3 inflammasome activation. Similar to results obtained with ATP-stimulated cells (Fig. 1c), MCC950 and glyburide inhibited nigericin-induced caspase-1 and IL-1 β processing (Fig. 3a). MCC950 did not alter the expression of pro-caspase-1, pro-IL-1 β or ASC in cell lysates (Fig. 3a). Cytosolic fractions from cell lysates were cross-linked, and ASC monomers and higher order complexes were observed after stimulation with LPS and nigericin. ASC-complex formation was attenuated by MCC950 and glyburide (Fig. 3a). ASC oligomerization was also observed when we used immortalized macrophages stably expressing ASC tagged with cerulean fluorescent protein. Upon NLRP3 activation by ATP, ASC-cerulean condenses into a large speck in each cell (Fig. 3b), but pretreatment with MCC950 inhibited speck formation (Fig. 3b). The relatively high concentration of MCC950 required to block speck formation in our assay might have been due to the nature of the cell line, which also stably expresses high levels of NLRP3 and thus does not require

Figure 4 MCC950 does not block K⁺ efflux, Ca²⁺ flux or direct NLRP3 and ASC interactions.

(a) The relative level of intracellular K⁺ determined by inductively coupled plasma optical emission spectrometry in *Nlrp3*^{-/-} BMDMs stimulated with LPS and nigericin, ATP and SiO₂ and treated with MCC950. (b) IL-1 β production (as measured by ELISA) from C57BL/6 BMDMs stimulated with LPS and nigericin, ATP and SiO₂. Data in a and b are presented as the mean \pm sd from triplicate measurements and are representative of three independent experiments. (c) A trace showing ATP-induced Ca²⁺ flux was measured using the FLIPR^{TETRA} system in C57BL/6 BMDMs stimulated with LPS and treated with MCC950. The results are representative of three independent experiments. RFU, relative fluorescence units. (d,e) The relative response to ATP-induced Ca²⁺ flux in C57BL/6 (d) and *Ice*^{-/-} (e) BMDMs stimulated with LPS and treated with MCC950 as measured using the FLIPR^{TETRA} system. Data are presented as the mean \pm sem and are representative of three independent experiments. (f,g) Western blots of cell lysates and FLAG-immunoprecipitation (IP) samples from HEK-293T cells transfected with FLAG-NLRP3, hemagglutinin (HA)-NLRP3, ASC or empty vector plasmids as indicated and treated with MCC950. The results presented are representative of three independent experiments. (h) The percentage of ASC-speck-containing live HEK-293T cells transfected with GFP-ASC and NLRP3-mCherry plasmids as indicated, treated with MCC950 and analyzed by FACS. Data are presented as the mean \pm sem from three independent experiments, each carried out in triplicate.



priming. ASC-cerulean cells were examined using a range of inflammasome ligands (Fig. 3c and Supplementary Fig. 7). The number of activated cells observed after stimulation with nigericin or the lysosomal destabilizer LeuLeu-OMe, which activates NLRP3 (ref. 33), was dose-dependently decreased by pretreatment with MCC950. Speck formation was not decreased by MCC950 in cells stimulated with the NLRP1 ligand lethal toxin³⁴, which indicates the selectivity of MCC950 for NLRP3 (Fig. 3c and Supplementary Fig. 7).

MCC950 does not block K⁺ efflux, Ca²⁺ flux or NLRP3–ASC interactions

We next sought to address the mechanism of action of MCC950. K⁺ efflux is a trigger common to all NLRP3 activators³⁵, and MCC950 is structurally related to sulfonyleurea drugs such as glyburide that are known to target ATP-sensitive K⁺ channels³⁶. MCC950 dose-dependently inhibited the release of IL-1 β induced by nigericin, ATP and SiO₂ in LPS-primed macrophages, but it did not prevent K⁺ efflux triggered by these stimuli (Fig. 4a,b). It has been demonstrated that activation of the NLRP1 inflammasome is blocked by high concentrations of extracellular K⁺ (ref. 37), and we found that MCC950 did not block NLRP1 activation (Fig. 3c). These data suggest that MCC950 inhibits NLRP3 activation downstream of K⁺ efflux.

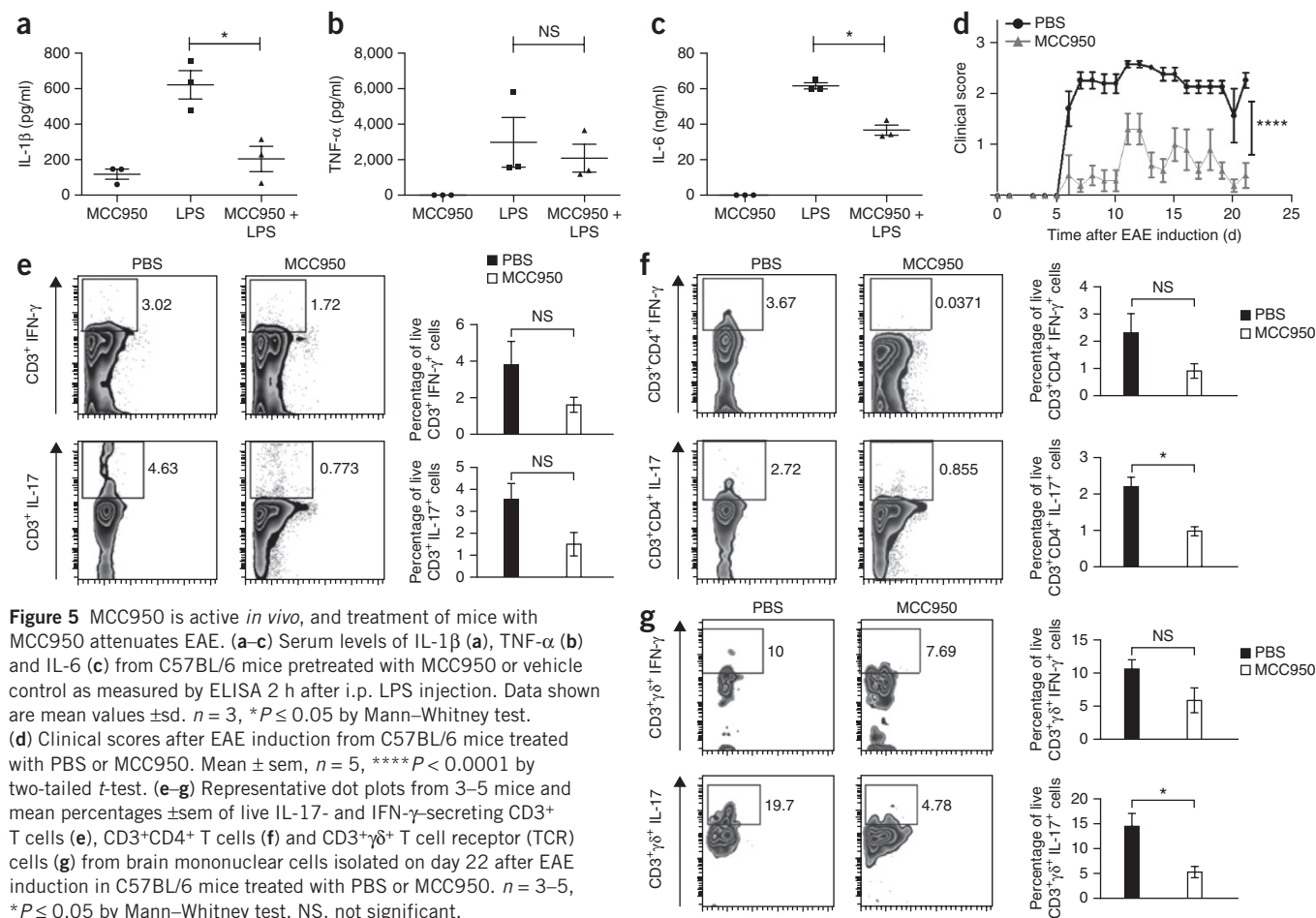
A requirement for Ca²⁺ signaling in the activation of NLRP3 was previously demonstrated³⁸. We examined whether MCC950 altered ATP-induced Ca²⁺ flux (Fig. 4c–e). *Ice*^{-/-} BMDMs were tested, as caspase-1 activation can lead to nonspecific membrane permeation and Ca²⁺ flux. Pretreatment with MCC950 in WT or *Ice*^{-/-} BMDMs

did not substantially affect the ATP-induced increase in intracellular Ca²⁺ (Fig. 4c–e), suggesting that MCC950 is unlikely to inhibit NLRP3 activation by modulating Ca²⁺ flux.

As we had observed that MCC950 could prevent NLRP3-induced ASC oligomerization, we next tested whether MCC950 could prevent direct NLRP3–NLRP3 or NLRP3–ASC interactions (Fig. 4f–h). HEK-293T cells were transfected with NLRP3 and ASC and treated with 50 μ M MCC950, and then a co-immunoprecipitation assay with NLRP3 was performed. MCC950 did not alter the interaction between NLRP3 and NLRP3 (Fig. 4f) or between NLRP3 and ASC (Fig. 4g). We also used a FACS-based assay to analyze GFP-tagged ASC speck formation induced by NLRP3 expression in a ligand-independent manner (Fig. 4h). Micromolar doses of MCC950 did not decrease the percentage of cells containing ASC specks. Although we cannot rule out the notion that MCC950 interacts directly with NLRP3, these data suggest that it does not prevent inflammasome formation by directly blocking NLRP3 oligomerization or NLRP3–ASC interactions.

MCC950 inhibits NLRP3 *in vivo* and attenuates EAE severity

We next investigated the effects of MCC950 *in vivo*. The induction of IL-1 β by intraperitoneal (i.p.) injection of LPS was shown to be NLRP3 dependent³⁹. We thus examined whether MCC950 could block this induction of IL-1 β . Mice were pretreated with MCC950 1 h before i.p. injection of LPS and were assessed 2 h later (Fig. 5a–c). Pretreatment with MCC950 reduced serum concentrations of IL-1 β and IL-6 but did not considerably decrease the amount of TNF- α , indicating that MCC950 is active *in vivo*.



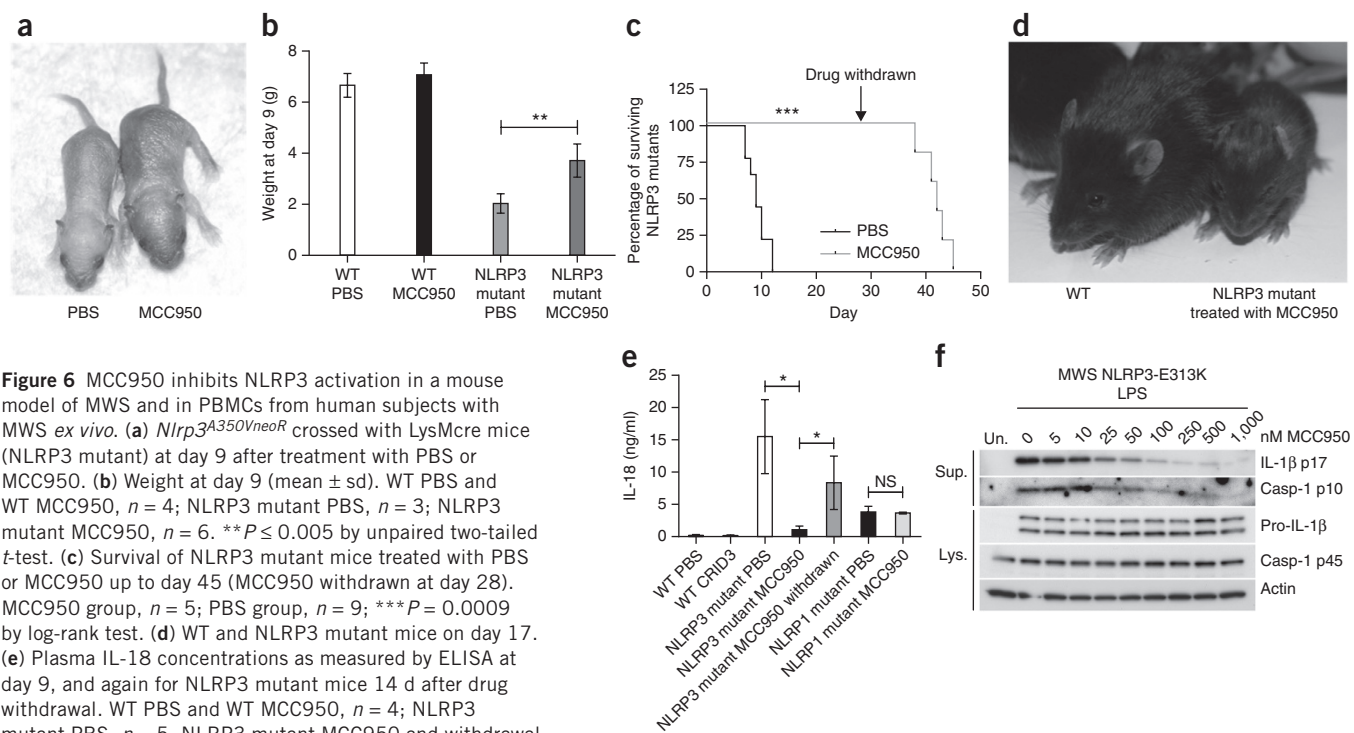


Figure 6 MCC950 inhibits NLRP3 activation in a mouse model of MWS and in PBMCs from human subjects with MWS *ex vivo*. (a) *Nlrp3*^{A350VneoR} crossed with *LysMcre* mice (NLRP3 mutant) at day 9 after treatment with PBS or MCC950. (b) Weight at day 9 (mean \pm sd). WT PBS and WT MCC950, $n = 4$; NLRP3 mutant PBS, $n = 3$; NLRP3 mutant MCC950, $n = 6$. $**P < 0.005$ by unpaired two-tailed *t*-test. (c) Survival of NLRP3 mutant mice treated with PBS or MCC950 up to day 45 (MCC950 withdrawn at day 28). MCC950 group, $n = 5$; PBS group, $n = 9$; $***P = 0.0009$ by log-rank test. (d) WT and NLRP3 mutant mice on day 17. (e) Plasma IL-18 concentrations as measured by ELISA at day 9, and again for NLRP3 mutant mice 14 d after drug withdrawal. WT PBS and WT MCC950, $n = 4$; NLRP3 mutant PBS, $n = 5$; NLRP3 mutant MCC950 and withdrawal, $n = 4$; *Nlrp1a*^{Q593P} (NLRP1 mutant) PBS and MCC950, $n = 3$. Data shown are the mean \pm sd. $*P \leq 0.05$ by Mann–Whitney test. (f) Western blots of cell lysates and supernatants from PBMCs isolated from an individual with MWS (mutation E313K), stimulated with LPS and treated with MCC950.

The effect of MCC950 in animal models of NLRP3-mediated diseases was then tested. The EAE mouse model is a model of the human disease multiple sclerosis. EAE is induced by immunization with a central nervous system autoantigen and causes T cell-mediated inflammation and demyelination. IL-1 signaling is crucial to the induction of IL-17 production from pathogenic CD4⁺ T helper 17 (T_H17) cells and $\gamma\delta$ ⁺ T cells^{40–42}. More recently it has been demonstrated that the development of EAE requires NLRP3 (ref. 43). We investigated the possibility that MCC950 may suppress T cell responses that mediate autoimmune disease. Treatment of mice with MCC950 delayed the onset and reduced the severity of EAE (Fig. 5d). Intracellular cytokine staining and FACS analysis of brain mononuclear cells from mice killed on day 22 after treatment showed modestly reduced frequencies of IL-17- and IFN- γ -producing CD3⁺ T cells in MCC950-treated mice in comparison with PBS-treated mice (Fig. 5e). Numbers of IFN- γ -cells, and particularly of IL-17-producing cells, were also reduced in both the CD4⁺ and $\gamma\delta$ ⁺ subpopulations of CD3⁺ T cells (Fig. 5f,g).

MCC950 is efficacious in a mouse model of CAPS and in cells from MWS subjects

A mouse model of the human CAPS MWS was generated by expression of the MWS-associated mutation *Nlrp3* (A350VneoR) (corresponding to *NLRP3* (A352V) in humans) specifically in the myeloid lineage (crossed with *LysMcre* mice)⁴⁴. NLRP3-mutant mice die in the neonatal period and have increased concentrations of circulating IL-1 β and IL-18 (ref. 44). We administered MCC950 to NLRP3-mutant mice (Fig. 6a) and observed that they had increased body weight at day 9 compared to PBS-treated controls (Fig. 6a,b). MCC950 treatment also increased survival up to days 38–45 even after treatment was stopped at day 28 (Fig. 6c,d). MCC950 treatment decreased the concentration of circulating IL-18 in

NLRP3-mutant mice; however, the concentration of IL-18 then increased after the withdrawal of MCC950 (Fig. 6e). A mouse strain containing an NLRP1-activating mutation (*Nlrp1a* (Q593P)) also displays increased concentrations of serum IL-18 relative to WT controls⁴⁵. However, treatment of NLRP1-mutant mice with MCC950 did not significantly alter serum concentrations of IL-18 (Fig. 6e) ($P = 0.7$). These data clearly demonstrate that MCC950 effectively and specifically blocks NLRP3 activation *in vivo*.

Finally we tested the effects of MCC950 in PBMCs from individuals with MWS, a CAPS caused by gain-of-function mutations in *NLRP3*, as mentioned above⁴⁶. PBMCs from individuals with MWS secrete IL-1 β in response to LPS alone, without an NLRP3 stimulus^{47,48}. When PBMCs from an individual with MWS were stimulated with LPS, caspase-1 and IL-1 β processing was detected in the cell supernatants (Fig. 6f). However, when cells were pretreated with MCC950, processing of both IL-1 β and caspase-1 was dose-dependently inhibited (Fig. 6f). MCC950 treatment did not alter the expression of pro-IL-1 β or pro-caspase-1 (Fig. 6f). Samples from four more individuals with MWS were also found to be sensitive to MCC950 inhibition (Supplementary Fig. 8). Thus, MCC950 inhibits NLRP3 inflammasome activation in samples from individuals with CAPS.

In vitro and *in vivo* pharmacokinetics of MCC950

To assess the therapeutic potential of MCC950, we examined the pharmacokinetic profile of this compound in a number of *in vitro* absorption, distribution, metabolism and excretion assays. The stability of MCC950 when incubated with human or mouse liver microsomes was good, with more than 70% of the compound remaining after 60 min (Supplementary Table 2). The drug–drug interaction potential of MCC950 was also tested (Supplementary Tables 3 and 4). MCC950 was incubated at a single concentration of 10 μ M with

human liver microsomes and a cocktail of standard substrates specific for each of the five major cytochrome P450 isozymes (1A2, 2C9, 2C19, 2D6 and 3A4). The inhibition of the five major cytochrome P450 enzymes by MCC950 was low, at less than 15% (**Supplementary Table 4**). To explore any potential for cardiotoxicity, we examined the effect of MCC950 on the human ether-a-go-go (hERG) potassium channel using the high-throughput automated patch clamp method (QPatch^{HTX}) (**Supplementary Table 5**). In this assay the IC₅₀ for hERG was greater than 30 μM, which suggests MCC950 has a >3,000-fold selectivity window (IC₅₀ for NLRP3 < 10 nM). Finally, a single-dose pharmacokinetic profile of MCC950 in C57BL/6 mice was determined via intravenous (3 mg kg⁻¹) and oral (20 mg kg⁻¹) administration of MCC950 (**Supplementary Fig. 9**). The area under the curve was 163,410 ng.h ml⁻¹, with a C_{max} of 25,333 ng ml⁻¹ and a half-life of 3.27 h. The oral bioavailability of MCC950 was 68%.

DISCUSSION

We describe here MCC950, a potent selective NLRP3 inhibitor that is active both in mice *in vivo* and in human cells *ex vivo*. MCC950 may be a useful tool for exploring NLRP3 biology and druggability.

We have characterized the mechanism of action of MCC950 in the context of our current understanding of NLRP3 activation. MCC950 did not block K⁺ efflux, Ca²⁺ flux or ligand-independent direct NLRP3 and ASC interactions. Reactive oxygen species have been implicated in NLRP3 activation, but current evidence suggests that they are not involved in activation by nigericin or by ATP^{38,49}, which were both potently inhibited by MCC950. MCC950 was active against the hypersensitive NLRP3 mutations associated with MWS, against noncanonical NLRP3 activation and against all tested canonical NLRP3 stimuli, which suggests that the molecular target of MCC950 is NLRP3 itself or is closely linked to the activation of NLRP3. It is possible that MCC950 binds to NLRP3 and affects a key step in its activation that might involve post-translational modification. Future work will aim to define the precise mechanism of action of MCC950.

We note that targeting NLRP3 might present certain advantages over the use of biologic inhibitors of IL-1β. MCC950 was effective in a genetic mouse model of CAPS (**Fig. 6a–e**). The rescue afforded by MCC950 is more substantial than the targeted blockade of IL-1β alone, which does not prevent lethality⁴⁴. Some of the pathology of this syndrome may be due to IL-18 and pyroptosis⁵⁰, which MCC950 will block. IL-1β maturation can be mediated by a number of different enzymes, including serine proteases and caspase-8 (ref. 3), and we have demonstrated that MCC950 does not block the major antimicrobial inflammasomes NLRC4 and NLRP1. Thus, specific targeting of NLRP3 will not result in the complete blockade of IL-1β *in vivo* during infection, and antimicrobial responses may remain intact. MCC950 may therefore have fewer immunosuppressive effects than biologics such as canakinumab, which has been shown clinically to increase the risk of these infections^{12,51}. MCC950 will also have a shorter half-life compared to the biologics canakinumab and riloncept and could therefore be withdrawn should unwanted effects such as infections occur. A small molecule such as MCC950 may also be more cost effective than biologic agents⁵². The future clinical development of MCC950 or derivatives may result in the development of new anti-inflammatory therapies for CAPS, but also of more complex diseases such as type 2 diabetes, multiple sclerosis and Alzheimer's disease.

METHODS

Methods and any associated references are available in the [online version of the paper](#).

Note: Any Supplementary Information and Source Data files are available in the online version of the paper.

ACKNOWLEDGMENTS

We thank A. Kitanovic (German Center for Neurodegenerative Diseases) for image analysis (**Fig. 3c**), S. Corr (Trinity College Dublin) for providing *S. typhimurium* UK-1 strain and H.M. Hoffman (University of California, San Diego) for providing *Nlrp3* (A350VneoR) mice. This work was supported by the following funding bodies, grants and fellowships. L.A.J.O'N. and R.C.C.: Science Foundation Ireland (G20598). D.L.K. and J.J.C.: Intramural Research Program of the National Human Genome Research Institute, US National Institutes of Health. S.C.H., C.E.S. and K.H.G.M.: Science Foundation Ireland (11/PI/1036) and (07/SRC/B1144). I.V.: Australian Research Council (FT130101215). G.N.: US National Institutes of Health (DK091191) and (DK095782). E.L.: German Research Foundation (SFB645, SFB670, SFB704, TRR57), European Research Council (ERC, InflammAct) and Excellence Cluster ImmunoSensation. S.L.M.: VESKI innovation fellowship and National Health and Medical Research Council of Australia (1032065) and (1057815). K.S.: Queensland Smart Futures Fund and Australian Research Council (FT130100361). L.A.J.O'N.: ERC Advanced Grant (E12435).

AUTHOR CONTRIBUTIONS

R.C.C. performed and analyzed the experiments described in **Figures 1b–j, 2, 3a,b and 4f–h** and **Supplementary Figure 6b–g**; helped analyze the experiments described in **Figure 5a–c** and **Supplementary Figure 6h,i**; and wrote the manuscript. A.A.B.R. synthesized MCC950, conducted formulation for *in vivo* studies, determined compound pharmacokinetics, helped write the manuscript and provided advice. J.J.C. performed the experiments described in **Figure 6f** and **Supplementary Figure 8**. S.C.H. performed and analyzed the experiment described in **Figure 5d–g**. R.M.–P. performed the experiments described in **Figure 4a,b**. M.C.I. and I.V. performed the experiments described in **Figure 4c–e**. L.S.D. performed the experiment described in **Figure 5a–c**. B.G.M. and A.S. performed the experiments described in **Figure 3c** and **Supplementary Figure 7**. D.E.C. performed the experiments described in **Supplementary Figure 6a**. M.S.B. performed the NMR analysis described in **Supplementary Figures 1–5** and **Supplementary Table 1**. M.H. performed the experiments described in **Supplementary Figure 6h,i**. C.E.S. helped analyze data from the experiment described in **Figure 5d–g**. G.N., E.L. and D.L.K. oversaw a portion of the work. K.H.G.M. conceived ideas and oversaw a portion of the work. S.L.M. performed and analyzed the experiments described in **Figure 6a–e**. K.S., S.L.M. and M.A.C. conceived ideas, oversaw a portion of the work, reviewed the manuscript and provided advice. L.A.J.O'N. conceived ideas, oversaw the research program and wrote the manuscript.

COMPETING FINANCIAL INTERESTS

The authors declare no competing financial interests.

Reprints and permissions information is available online at <http://www.nature.com/reprints/index.html>.

- Wen, H., Miao, E.A. & Ting, J.P. Mechanisms of NOD-like receptor-associated inflammasome activation. *Immunity* **39**, 432–441 (2013).
- Schroder, K. & Tschopp, J. The inflammasomes. *Cell* **140**, 821–832 (2010).
- Latz, E., Xiao, T.S. & Stutz, A. Activation and regulation of the inflammasomes. *Nat. Rev. Immunol.* **13**, 397–411 (2013).
- Lamkanfi, M. & Dixit, V.M. Mechanisms and functions of inflammasomes. *Cell* **157**, 1013–1022 (2014).
- Masters, S.L., Simon, A., Aksentijevich, I. & Kastner, D.L. Horror autinflammaticus: the molecular pathophysiology of autoinflammatory disease. *Annu. Rev. Immunol.* **27**, 621–668 (2009).
- Wen, H., Ting, J.P. & O'Neill, L.A. A role for the NLRP3 inflammasome in metabolic diseases: did Warburg miss inflammation? *Nat. Immunol.* **13**, 352–357 (2012).
- De Nardo, D., De Nardo, C.M. & Latz, E. New insights into mechanisms controlling the NLRP3 inflammasome and its role in lung disease. *Am. J. Pathol.* **184**, 42–54 (2014).
- Szabo, G. & Csak, T. Inflammasomes in liver diseases. *J. Hepatol.* **57**, 642–654 (2012).
- Anders, H.J. & Muruve, D.A. The inflammasomes in kidney disease. *J. Am. Soc. Nephrol.* **22**, 1007–1018 (2011).
- Youm, Y.H. *et al.* Canonical *Nlrp3* inflammasome links systemic low-grade inflammation to functional decline in aging. *Cell Metab.* **18**, 519–532 (2013).

11. Masters, S.L. *et al.* Activation of the NLRP3 inflammasome by islet amyloid polypeptide provides a mechanism for enhanced IL-1 β in type 2 diabetes. *Nat. Immunol.* **11**, 897–904 (2010).
12. Dinarello, C.A. & van der Meer, J.W. Treating inflammation by blocking interleukin-1 in humans. *Semin. Immunol.* **25**, 469–489 (2013).
13. Lamkanfi, M. *et al.* Glyburide inhibits the Cryopyrin/Nalp3 inflammasome. *J. Cell Biol.* **187**, 61–70 (2009).
14. Coll, R.C., Robertson, A., Butler, M., Cooper, M. & O'Neill, L.A. The cytokine release inhibitory drug CRID3 targets ASC oligomerisation in the NLRP3 and AIM2 inflammasomes. *PLoS ONE* **6**, e29539 (2011).
15. Juliana, C. *et al.* Anti-inflammatory compounds parthenolide and Bay 11–7082 are direct inhibitors of the inflammasome. *J. Biol. Chem.* **285**, 9792–9802 (2010).
16. He, Y. *et al.* 3,4-Methylenedioxy- β -nitrostyrene inhibits NLRP3 inflammasome activation by blocking assembly of the inflammasome. *J. Biol. Chem.* **289**, 1142–1150 (2014).
17. Ahn, H., Kim, J., Jeung, E.B. & Lee, G.S. Dimethyl sulfoxide inhibits NLRP3 inflammasome activation. *Immunobiology* **219**, 315–322 (2014).
18. Perregaux, D.G. *et al.* Identification and characterization of a novel class of interleukin-1 post-translational processing inhibitors. *J. Pharmacol. Exp. Ther.* **299**, 187–197 (2001).
19. Laliberte, R.E. *et al.* Glutathione S-transferase omega 1-1 is a target of cytokine release inhibitory drugs and may be responsible for their effect on interleukin-1 β post-translational processing. *J. Biol. Chem.* **278**, 16567–16578 (2003).
20. Mariathasan, S. *et al.* Cryopyrin activates the inflammasome in response to toxins and ATP. *Nature* **440**, 228–232 (2006).
21. Martinon, F., Petrilli, V., Mayor, A., Tardivel, A. & Tschopp, J. Gout-associated uric acid crystals activate the NALP3 inflammasome. *Nature* **440**, 237–241 (2006).
22. Groß, O. *et al.* Inflammasome activators induce interleukin-1 α secretion via distinct pathways with differential requirement for the protease function of caspase-1. *Immunity* **36**, 388–400 (2012).
23. Jin, C. *et al.* NLRP3 inflammasome plays a critical role in the pathogenesis of hydroxyapatite-associated arthropathy. *Proc. Natl. Acad. Sci. USA* **108**, 14867–14872 (2011).
24. Netea, M.G. *et al.* Differential requirement for the activation of the inflammasome for processing and release of IL-1 β in monocytes and macrophages. *Blood* **113**, 2324–2335 (2009).
25. Kayagaki, N. *et al.* Non-canonical inflammasome activation targets caspase-11. *Nature* **479**, 117–121 (2011).
26. Kayagaki, N. *et al.* Noncanonical inflammasome activation by intracellular LPS independent of TLR4. *Science* **341**, 1246–1249 (2013).
27. Broz, P., von Moltke, J., Jones, J.W., Vance, R.E. & Monack, D.M. Differential requirement for caspase-1 autoproteolysis in pathogen-induced cell death and cytokine processing. *Cell Host Microbe* **8**, 471–483 (2010).
28. Bürckstümmer, T. *et al.* An orthogonal proteomic-genomic screen identifies AIM2 as a cytoplasmic DNA sensor for the inflammasome. *Nat. Immunol.* **10**, 266–272 (2009).
29. Hornung, V. *et al.* AIM2 recognizes cytosolic dsDNA and forms a caspase-1-activating inflammasome with ASC. *Nature* **458**, 514–518 (2009).
30. Fernandes-Alnemri, T., Yu, J.W., Datta, P., Wu, J. & Alnemri, E.S. AIM2 activates the inflammasome and cell death in response to cytoplasmic DNA. *Nature* **458**, 509–513 (2009).
31. Roberts, T.L. *et al.* HIN-200 proteins regulate caspase activation in response to foreign cytoplasmic DNA. *Science* **323**, 1057–1060 (2009).
32. Kwok, B.H., Koh, B., Ndubuisi, M.I., Elofsson, M. & Crews, C.M. The anti-inflammatory natural product parthenolide from the medicinal herb Feverfew directly binds to and inhibits I κ B kinase. *Chem. Biol.* **8**, 759–766 (2001).
33. Hornung, V. *et al.* Silica crystals and aluminum salts activate the NALP3 inflammasome through phagosomal destabilization. *Nat. Immunol.* **9**, 847–856 (2008).
34. Boyden, E.D. & Dietrich, W.F. Nalp1b controls mouse macrophage susceptibility to anthrax lethal toxin. *Nat. Genet.* **38**, 240–244 (2006).
35. Muñoz-Planillo, R. *et al.* K⁺ efflux is the common trigger of NLRP3 inflammasome activation by bacterial toxins and particulate matter. *Immunity* **38**, 1142–1153 (2013).
36. Ashcroft, F.M. ATP-sensitive potassium channelopathies: focus on insulin secretion. *J. Clin. Invest.* **115**, 2047–2058 (2005).
37. Petrilli, V. *et al.* Activation of the NALP3 inflammasome is triggered by low intracellular potassium concentration. *Cell Death Differ.* **14**, 1583–1589 (2007).
38. Horg, T. Calcium signaling and mitochondrial destabilization in the triggering of the NLRP3 inflammasome. *Trends Immunol.* **35**, 253–261 (2014).
39. He, Y., Franchi, L. & Nunez, G. TLR agonists stimulate Nlrp3-dependent IL-1 β production independently of the purinergic P2X7 receptor in dendritic cells and *in vivo*. *J. Immunol.* **190**, 334–339 (2013).
40. Lalor, S.J. *et al.* Caspase-1-processed cytokines IL-1 β and IL-18 promote IL-17 production by $\gamma\delta$ and CD4 T cells that mediate autoimmunity. *J. Immunol.* **186**, 5738–5748 (2011).
41. Sutton, C., Brereton, C., Keogh, B., Mills, K.H. & Lavelle, E.C. A crucial role for interleukin (IL)-1 in the induction of IL-17-producing T cells that mediate autoimmune encephalomyelitis. *J. Exp. Med.* **203**, 1685–1691 (2006).
42. Sutton, C.E. *et al.* Interleukin-1 and IL-23 induce innate IL-17 production from $\gamma\delta$ T cells, amplifying Th17 responses and autoimmunity. *Immunity* **31**, 331–341 (2009).
43. Gris, D. *et al.* NLRP3 plays a critical role in the development of experimental autoimmune encephalomyelitis by mediating Th1 and Th17 responses. *J. Immunol.* **185**, 974–981 (2010).
44. Brydges, S.D. *et al.* Inflammasome-mediated disease animal models reveal roles for innate but not adaptive immunity. *Immunity* **30**, 875–887 (2009).
45. Masters, S.L. *et al.* NLRP1 inflammasome activation induces pyroptosis of hematopoietic progenitor cells. *Immunity* **37**, 1009–1023 (2012).
46. Hoffman, H.M., Mueller, J.L., Broide, D.H., Wanderer, A.A. & Kolodner, R.D. Mutation of a new gene encoding a putative pyrin-like protein causes familial cold autoinflammatory syndrome and Muckle-Wells syndrome. *Nat. Genet.* **29**, 301–305 (2001).
47. Gattorno, M. *et al.* Pattern of interleukin-1 β secretion in response to lipopolysaccharide and ATP before and after interleukin-1 blockade in patients with CIAS1 mutations. *Arthritis Rheum.* **56**, 3138–3148 (2007).
48. Lee, G.S. *et al.* The calcium-sensing receptor regulates the NLRP3 inflammasome through Ca²⁺ and cAMP. *Nature* **492**, 123–127 (2012).
49. Bauernfeind, F. *et al.* Cutting edge: reactive oxygen species inhibitors block priming, but not activation, of the NLRP3 inflammasome. *J. Immunol.* **187**, 613–617 (2011).
50. Brydges, S.D. *et al.* Divergence of IL-1, IL-18, and cell death in NLRP3 inflammasomopathies. *J. Clin. Invest.* **123**, 4695–4705 (2013).
51. López-Castejón, G. & Pelegrin, P. Current status of inflammasome blockers as anti-inflammatory drugs. *Expert Opin. Investig. Drugs* **21**, 995–1007 (2012).
52. Fautrel, B. Economic benefits of optimizing anchor therapy for rheumatoid arthritis. *Rheumatology (Oxford)* **51** (suppl. 4), iv21–iv26 (2012).

ONLINE METHODS

MCC950 synthesis and formulation. MCC950 was synthesized via a ten-step route⁵³. The 1,2,3,5,6,7-hexahydro-*s*-indacen-4-amine moiety was synthesized from 2,3-dihydro-1H-indene such that Friedel–Crafts acylation using 3-chloropropionyl chloride and aluminum trichloride in dichloromethane gave 3-chloro-1-(2,3-dihydro-1H-inden-5-yl)propan-1-one, which was not purified and was used directly in the cyclization reaction. Cyclization was achieved by heating the crude product to 60 °C in concentrated sulfuric acid for 72 h and then cooling the solution to 0 °C and nitrating it directly using a 1:1 mixture of nitric and sulfuric acids. After trituration with ice-cold methanol, a regioisomeric mixture of 4-nitro- and 8-nitro-3,5,6,7-tetrahydro-*s*-indacen-1(2H)-one was isolated in 61% yield over the three synthetic steps. Simultaneous reduction of the ketone and nitro groups was successfully achieved by hydrogenation in methanol over Pearlman's catalyst in the presence of methanesulfonic acid in 62% yield after purification by column chromatography on silica.

The required 4-(2-hydroxypropan-2-yl)furan-2-sulfonamide moiety was synthesized from ethyl furan-3-carboxylate. Sulfonylation of the furan-5 position was readily achieved using chlorosulfonic acid in dichloromethane in the temperature range from –10 °C to room temperature. The 4-(ethoxycarbonyl)furan-2-sulfonic acid intermediate was not isolated and instead was chlorinated directly by the addition of pyridine and phosphorous pentachloride to the reaction mixture. After work-up and silica column chromatography, ethyl 5-(chlorosulfonyl)furan-3-carboxylate was isolated in 56% yield over the two steps. The chloride was displaced using ammonium bicarbonate in water and acetone to yield 4-(2-hydroxypropan-2-yl)furan-2-sulfonamide in 59% yield after aqueous work-up. The sulfonamide was pure enough to use in the next reaction step, where the ester moiety was reduced using methylmagnesium chloride in tetrahydrofuran to the tertiary alcohol, giving 4-(2-hydroxypropan-2-yl)furan-2-sulfonamide in 53% yield.

To complete the synthesis of MCC950, we converted the 1,2,3,5,6,7-hexahydro-*s*-indacen-4-amine to the corresponding isocyanate by reaction with di-*tert*-butyl dicarbonate and *N,N*-dimethylaminopyridine in acetonitrile. The sodium salt of 4-(2-hydroxypropan-2-yl)furan-2-sulfonamide was prepared by reaction with freshly prepared sodium methoxide solution, and the solvent was removed *in vacuo* to give a hygroscopic sodium salt. The salt was suspended in acetonitrile, the preformed isocyanate solution was added and the reaction was stirred overnight. MCC950 sodium salt was filtered directly from the reaction mixture, and the beige solid was triturated using ethyl acetate. The product was dissolved in water, treated with activated charcoal and filtered through Celite. The aqueous solution was freeze-dried to give the desired product as the sodium salt.

Spectra of MCC950 and intermediates were consistent with the literature⁵³ and results of electrospray ionization high-resolution mass spectrometry (exact mass calculated for MCC950 C₂₀H₂₃N₂O₅S (M–H⁺), 403.1333; found, 403.1351. MCC950 sodium salt is highly soluble in aqueous solutions and therefore was formulated in saline for *in vivo* studies.

Cell culture. Bone marrow from C57BL/6, *Nlrp3*^{–/–} (ref. 21), *Ice*^{–/–} (ref. 54) and *Casp11*^{–/–} (ref. 55) mice was differentiated for 7 d in DMEM supplemented with 10% FCS, 1% penicillin/streptomycin (P/S) and 20% L929 mouse fibroblast supernatant or in RPMI 1640 medium supplemented with 10% FCS, 1% P/S and 10 ng/ml human macrophage colony-stimulating factor (M-CSF) (ImmunoTools). Stably transfected ASC-cerulean macrophages as described by Hett *et al.*⁵⁶ were cultured in DMEM supplemented with 10% FCS and 1% P/S. HEK-293T cells were cultured in DMEM supplemented with 10% FCS and 1% P/S. Blood specimens from individuals with CAPS were drawn after informed consent had been obtained under a protocol approved by the National Institute of Arthritis and Musculoskeletal and Skin Diseases/National Institute of Diabetes and Digestive and Kidney Diseases Institutional Review Board. Human PBMCs were isolated from freshly drawn peripheral venous blood with LSM-Lymphocyte Separation Medium (catalog no. 50494, MP Biomedicals). PBMCs were cultured in RPMI 1640 medium containing 10% FCS and antibiotics. HMDMs were generated from CD14⁺ monocytes by differentiation for 7 d in IMDM supplemented with 10% FCS, 1% P/S and 10 ng/ml human M-CSF (Miltenyi Biotec) as described by Croker *et al.*⁵⁷.

Inflammasome activation assays. We seeded BMDMs at 5 × 10⁵/ml or 1 × 10⁶/ml, HMDMs at 5 × 10⁵/ml and PBMCs at 2 × 10⁶/ml or 5 × 10⁶/ml

in 96-well plates. The following day, the overnight medium was replaced and cells were stimulated with 10 ng/ml LPS from *Escherichia coli* serotype EH100 (ra) TLRgrade (Alexis Biochemicals) for 3 h. The medium was removed and replaced with serum-free medium (SFM) containing DMSO (1:1,000), MCC950 (0.001–10 μM), glyburide (200 μM) (Sigma-Aldrich), parthenolide (10 μM) (Enzo Life Sciences) or Bayer cysteinyl leukotriene-receptor antagonist 1-(5-carboxy-2-[3-[4-(3-cyclohexylpropoxy)phenyl]propoxy]benzoyl)piperidine-4-carboxylic acid (40 μM) (Amgen) for 30 min. Cells were then stimulated with the following inflammasome activators: 5 mM adenosine 5'-triphosphate disodium salt hydrate (ATP) (1 h), 1 μg/ml poly(deoxyadenylic-thymidylic) acid sodium salt (Poly dA:dT) (Sigma-Aldrich) transfected with Lipofectamine 2000 (Invitrogen) (3–4 h), 200 μg/ml MSU (overnight) and 10 μM nigericin (Invivogen) (1 h) or *S. typhimurium* UK-1 strain (multiplicity of infection (MOI) (2 h). Cells were also stimulated with 25 μg/ml polyadenylic-polyuridylic acid (Invivogen) (4 h). For noncanonical inflammasome activation, cells were primed with 100 ng/ml Pam3CSK4 (Invivogen) for 4 h, after which the medium was removed and replaced with SFM containing DMSO or MCC950 and 2 μg/ml LPS was transfected using 0.25% FuGENE (Promega) for 16 h. Supernatants were removed and analyzed using ELISA kits according to the manufacturer's instructions (DuoSet, R&D Systems or ReadySetGo!, eBioscience). LDH release was measured using the CytoTox96 nonradioactive cytotoxicity assay (Promega).

Western blotting. Cell lysates were prepared by direct lysis in 50 μl of 5× Laemmli sample buffer. The protein content of supernatants was concentrated using StrataClean resin (Agilent Technologies) according to the manufacturer's instructions. The protein samples were resolved on 15% SDS-PAGE gels and transferred onto polyvinylidene difluoride membrane using a wet-transfer system. Membranes were blocked in 5% (wt/vol) dried milk in TBS-T (50 mM Tris/HCL, pH 7.6, 150 mM NaCl and 0.1% (vol/vol) Tween-20) for 1 h at room temperature. Membranes were incubated with primary antibody diluted in 5% (wt/vol) dried milk in TBS-T and then with the appropriate horseradish peroxidase (HRP)-conjugated secondary antibody diluted in 5% (wt/vol) dried milk in TBS-T for 1 h. Membranes were developed using 20× LumiGLO chemiluminescent reagent (Cell Signaling Technology). Membranes were stripped using Restore PLUS western blot stripping buffer (Thermo Fisher Scientific) before being re-probed.

PBMCs from individuals with CAPS were seeded at 2 × 10⁶/ml in 12-well plates and then primed with 1 μg/ml LPS for 3 h. The medium was replaced with SFM containing MCC950 (5–1,000 nM). After 45 min, cell culture supernatants and cell lysates were collected. Samples were resolved using Novex Tris-Glycine Gel Systems (Invitrogen).

Primary antibodies used were ASC antibody (AL177) (1 in 1,000) (Enzo Life Sciences); β-actin (AC-74) (1:10,000), FLAG M2 (F1804) (1:2,500) and α-tubulin clone B-5-1-2 (T5168) (1:5,000) (Sigma-Aldrich); mouse caspase-1 p10 (sc-514) (1:1,000), human caspase-1 p10 (sc-515) (1:1,000), human procaspase-1 (sc-622) (1:1,000) and human actin (sc-1615) (1:1,000) (Santa Cruz Biotechnology); mouse IL-1β (AB-401-NA) (1:1,000) and human IL-1β (AF-201-NA) (1:1,000) (R&D Systems); HA.11 clone 16B12 (MMS-101R) (1:2,000) (Covance); and NLRP3 clone Cryo-2 (AG-20B-0014) (1:1,000) (Adipogen). Secondary HRP-conjugated antibodies used were anti-mouse IgG, anti-rabbit IgG and anti-goat IgG (all 1:1,000) (Jackson ImmunoResearch).

ASC-complex isolation. BMDMs were seeded at 10⁶/ml in six-well plates. The following day, the medium was replaced and cells were stimulated with 10 ng/ml LPS for 3 h. The medium was removed and replaced with SFM containing the indicated inhibitors or controls for 30 min, followed by the addition of 10 μM nigericin for 1 h. The supernatants were removed, cells were rinsed in ice-cold PBS, and 500 μl of ice-cold buffer (20 mM HEPES-KOH, pH 7.5, 150 mM KCL, 1% NP-40, 0.1 mM PMSF, 1 mg/ml leupeptin, 11.5 mg/ml aprotinin and 1 mM sodium orthovanadate) was added. Cells were scraped and lysed by being sheared ten times through a 21-gauge needle. 50 μl of lysate was removed for western blot analysis. Lysates were centrifuged at 330 × *g* for 10 min at 4 °C. The pellets were washed twice in 1 ml of ice-cold PBS and resuspended in 500 μl of PBS. 2 mM disuccinimidyl suberate (DSS) (from a fresh 100 mM stock prepared from DSS equilibrated to room temperature and made up in dry DMSO) was added to the resuspended pellets, which were incubated at room temperature for 30 min with rotation. Samples were then centrifuged at 330 × *g* for 10 min at 4 °C. The supernatant was removed, and the cross-linked pellets were

resuspended in 30 μ l of Laemmli sample buffer. Samples were boiled for 5 min at 99 °C and analyzed by western blotting.

Confocal microscopy. For confocal images, ASC-cerulean cells were seeded at 2×10^5 /ml the day before use in experiments on 35 mm glass-bottom culture dishes. The following day the overnight medium was replaced with SFM containing the indicated inhibitors or controls for 30 min. Cells were then stimulated with 5 mM ATP for 30 min. Imaging was performed on an Olympus FluoView FV1000 Microscope equipped with a temperature- and CO₂-controlled chamber. For quantification of ASC speck formation, ASC-cerulean cells were seeded at 3.75×10^5 /ml the day before use in experiments in 384-well plates. The next day MCC950 was added using an HP compound printer, and 1 h later the following activators were added: 10 μ M nigericin (1.5 h), 1 mM LeuLeu-OMe (2 h) and 1 μ g/ml lethal toxin (1 μ g/ml lethal factor plus 1 μ g/ml protective antigen) (2 h). A solution of DRAQ5 (1:1,000) and 1% formaldehyde were added, and the plates were quantitated as described by Hett *et al.*⁵⁶.

K⁺ analysis. Intracellular K⁺ measurements were performed by inductively coupled plasma optical emission spectrometry with a PerkinElmer Optima 2000 DV spectrometer using yttrium as the internal standard as described by Muñoz-Planillo *et al.*³⁵. Cells were stimulated with 500 ng/ml LPS for 3 h, treated with MCC950 (10–300 nM) and then stimulated with 10 μ M nigericin or 5 mM ATP for 30 min or 375 μ g/ml SiO₂ for 6 h.

Fluorescence imaging plate reader Ca²⁺ analysis. BMDMs (3×10^4 /well) were loaded for 30 min at 37 °C with a no-wash calcium dye (Molecular Devices) in physiological salt solution (composition: NaCl, 140 mM; glucose, 11.5 mM; KCl, 5.9 mM; MgCl₂, 1.4 mM; NaH₂PO₄, 1.2 mM; NaHCO₃, 5 mM; CaCl₂, 1.8 mM; HEPES, 10 mM) containing 0.1% BSA. Cells were then transferred to the FLIPR^{TETRA} (Molecular Devices) fluorescent plate reader, and Ca²⁺ responses were measured using a cooled CCD (charge-coupled device) camera with excitation at 470–495 nM and emission at 515–575 nM. Camera gain and intensity were adjusted for each plate to yield a minimum baseline fluorescence of 1,000 arbitrary fluorescence units. Prior to the addition of MCC950, 10 baseline fluorescence readings were taken, followed by fluorescent readings every second for 300 s following sample addition and for a further 300 s following the addition of either physiological salt solution or ATP (500 μ M).

Co-immunoprecipitation assay. HEK-293T cells (3×10^5 /ml) were transfected in 10 cm² dishes via the calcium phosphate method with the following plasmids: pEF6 mouse NLRP3 N-HA, pEF6 mouse ASC, pEF6 mouse NLRP3 N-FLAG and empty vector control. 24 h after transfection, cells were lysed in RIPA buffer (50 mM Tris-HCL, pH 8, 150 mM NaCl, 1 mM EDTA, 10% glycerol, 1% Triton X-100, 1% sodium deoxycholate, 0.1% SDS and protease inhibitors) and disrupted by passage through a 27-gauge needle. Lysates were precleared with 5 μ l of protein G Dynabeads (Life Technologies) for 30 min at 4 °C. Dynabeads were blocked in 0.5% BSA for 1 h at 4 °C. Lysates were incubated for 1 h with 0.5 μ g anti-FLAGM2 (F1804) (Sigma-Aldrich) antibody before the addition of 20 μ l of blocked Dynabeads for a further 2 h at 4 °C. Dynabeads were captured using a magnet, washed and resuspended in 60 μ l of sample buffer and boiled for 5 min before analysis by western blotting.

Time-of-flight inflammasome evaluation assay. HEK-293T cells (4×10^5 /ml) were transfected in 24-well plates using Lipofectamine 2000 (Invitrogen) with the following plasmids: pEF6 human ASC-GFP, pEF6 human C-mCherry and empty vector control. 1 h post-transfection, cells were treated with DMSO or MCC950 (0.1–50 μ M). 15 h after transfection, cells were removed and suspended in Dulbecco's PBS containing 1% FCS and 2 mM EDTA. Cells were analyzed using a Gallios flow cytometer (Beckman Coulter) and using FlowJo software. Live cells were gated on GFP and mCherry expression (when co-transfected). We determined the percentage of cells containing ASC specks by analyzing the height and width of the GFP pulse area (low width:area and high height:area). This analysis is described in detail in by Sester *et al.*⁵⁸.

In vivo LPS challenge. C57BL/6 mice were injected intraperitoneally with 50 mg/kg MCC950 or vehicle control (DMSO/PBS) 1 h before i.p. injection of 10 mg/kg LPS *Escherichia coli* 055:B5 (Sigma-Aldrich) or PBS. After 2 h mice were killed, and serum levels of IL-1 β , TNF- α and IL-6 were measured by ELISA.

Induction and assessment of EAE. C57BL/6 mice were immunized subcutaneously with 150 μ g of MOG peptide 35-55 (GenScript) emulsified in complete Freund's adjuvant containing 4 mg/ml (0.4 mg/mouse) of heat-killed *Mycobacterium tuberculosis* (Chondrex). Mice were injected intraperitoneally with 500 ng pertussis toxin (Kaketsuken) on days 0 and 2. MCC950 was administered intraperitoneally to mice (10 mg/kg) at induction of the disease; on days 0, 1 and 2; and every 2 d thereafter. Control mice were administered vehicle (PBS) at the same time points. Mice were observed for clinical signs of disease daily (unblinded). Disease severity was scored as follows: no clinical signs, 0; limp tail, 1; ataxic gait, 2; hind limb weakness, 3; hind limb paralysis, 4; and tetraparalysis, 5. Experiments were performed under license (B100/2412) from the Irish Medicine Board and with approval from the Trinity College Dublin BioResources Ethics Committee.

FACS analysis of EAE. On day 22 post-immunization, mononuclear cells (MNCs) were isolated from whole brains of perfused mice with EAE, following homogenization and centrifugation on a Percoll gradient. MNCs (2×10^6 /ml) were stimulated for 4 h with phorbol 12-myristate 13-acetate (10 ng/ml) and ionomycin (1 μ g/ml) in the presence of brefeldin A (5 μ g/ml). Cells were washed in PBS and resuspended in 50 μ l of PBS with a 1:1,000 LIVE/DEAD Fixable Aqua Dead Cell Stain kit (Life Technologies) for 20 min. Surface stains for CD3 (145-2c11) (0.5 μ l/10⁶ cells), CD4 (RM4-5) (0.5 μ l/10⁶ cells) and γ δ TCR (GL3) (1 μ l/10⁶ cells) (eBioscience) were added, and cells were incubated for an additional 20 min. Cells were then fixed with 2% paraformaldehyde and washed in PBS twice before being intracellularly stained for IL-17 or IFN- γ in permeabilization buffer (0.2% saponin in PBS + 1% FBS). Flow cytometric analysis of MNCs was performed using a BD LSRFortessa (BD Biosciences), and results were analyzed with FlowJo software. MNCs were gated first on live CD3⁺ T cells followed by CD4 expression, γ δ TCR expression or cytokine production.

NLRP3- and NLRP1-activating mutations in mice. NLRP3- and NLRP1-activating mutations in mice were backcrossed to C57BL/6 at least ten times. *Nlrp3* (A350VneoR) mice were crossed with LysMcre mice (B6.129P2-*Lyz2*^{tm1(cre)lfo}/J). MCC950 was administered intraperitoneally (20 mg/kg) every second day starting at day 4 after birth. Mice with an activating mutation in NLRP1 (*Nlrp1a* (Q593P)) were generated on a C57BL/6 background as described previously⁴⁵ and administered MCC950 intraperitoneally (20 mg/kg) every second day for 9 d. Blood was collected at the time points indicated for analysis of plasma cytokines by ELISA. IL-18 ELISA was performed as described by Westwell-Roper *et al.*⁵⁹. Experiments were performed under AEC Project 2013.011 and were approved by the Animal Ethics Committee of the Walter and Eliza Hall Institute of Medical Research.

Statistical analyses. Data are presented as average values \pm sem from multiple individual experiments each carried out in triplicate or as average values \pm sd from triplicate measurements in a representative experiment. Nonlinear regression analysis of inhibitor versus normalized response (variable slope) was performed using Prism Software (GraphPad). Statistical analysis was carried out using a nonparametric Mann-Whitney *t*-test, an unpaired two-tailed *t*-test, or a log-rank test using Prism software (GraphPad). Data were considered significant when $P \leq 0.05$ (*), $P \leq 0.01$ (**), $P \leq 0.001$ (***) or $P \leq 0.0001$ (****).

- Urban, F.J. *et al.* Novel synthesis of 1-(1,2,3,5,6,7-hexahydro-s-indacen-4-yl)-3-[4-(1-hydroxy-1-methyl-ethyl)-furan-2-sulfonyl]urea, an anti-inflammatory agent. *Synth. Commun.* **33**, 2029–2043 (2003).
- Kuida, K. *et al.* Altered cytokine export and apoptosis in mice deficient in interleukin-1 β converting enzyme. *Science* **267**, 2000–2003 (1995).
- Wang, S. *et al.* Murine caspase-11, an ICE-interacting protease, is essential for the activation of ICE. *Cell* **92**, 501–509 (1998).
- Hett, E.C. *et al.* Chemical genetics reveals a kinase-independent role for protein kinase R in pyroptosis. *Nat. Chem. Biol.* **9**, 398–405 (2013).
- Crocker, D.E. *et al.* C5a2 can modulate ERK1/2 signaling in macrophages via heteromer formation with C5a1 and β -arrestin recruitment. *Immunol. Cell Biol.* **92**, 631–639 (2014).
- Sester, D.P. *et al.* A novel flow cytometric method to assess inflammasome formation. *J. Immunol.* **194**, 455–462 (2015).
- Westwell-Roper, C., Dunne, A., Kim, M.L., Verchere, C.B. & Masters, S.L. Activating the NLRP3 inflammasome using the amyloidogenic peptide IAPP. *Methods Mol. Biol.* **1040**, 9–18 (2013).